

Upgrade of the MAGIC telescopes

DANIEL MAZIN^{1,2}, DIEGO TESCARO^{2,3,5}, MARKUS GARCZARCZYK⁴, GIANLUCA GIAVITTO^{2,6}, JULIAN SITAREK²
FOR THE MAGIC COLLABORATION.

¹ Max-Planck-Institut für Physik, D-80805 München, Germany

² IFAE, Edifici Cn., Campus UAB, E-08193 Bellaterra, Spain

³ INFN Pisa, I-56127 Pisa, Italy

⁴ Deutsches Elektronen-Synchrotron (DESY), D-15738 Zeuthen, Germany

⁵ now at: Inst. de Astrofísica de Canarias, E-38200 La Laguna, and Universidad de La Laguna (ULL), Dept. Astrofísica, E-38206 La Laguna, Tenerife, Spain

⁶ now at: Deutsches Elektronen-Synchrotron (DESY), D-15738 Zeuthen, Germany.

mazin@mpp.mpg.de

Abstract: The MAGIC telescopes are two Imaging Atmospheric Cherenkov Telescopes (IACTs) located on the Canary island of La Palma. With 17m diameter mirror dishes and ultra-fast electronics, they provide an energy threshold as low as 50 GeV for observations at low zenith angles. The first MAGIC telescope was taken in operation in 2004 whereas the second one joined in 2009. In 2011 we started a major upgrade program to improve and to unify the stereoscopic system of the two similar but at that time different telescopes. Here we report on the upgrade of the readout electronics and digital trigger of the two telescopes, the upgrade of the camera of the MAGIC I telescope as well as the commissioning of the system after this major upgrade.

Keywords: MAGIC, Cherenkov telescopes, gamma-ray astronomy, acquisition systems, trigger



Figure 1: The two 17m diameter MAGIC telescope system operating at the Roque de los Muchachos observatory in La Palma. The front telescope is the MAGIC II.

1 Introduction

The MAGIC telescopes (see Fig. 1) is a stereoscopic system of two Imaging Atmospheric Cherenkov Telescopes (IACTs) located at the observatory of Roque de los Muchachos in La Palma, Canary Islands. The telescopes are designed to observe very high energy gamma rays at energies between 50 GeV and tens of TeVs. The two MAGIC telescopes have been constructed 5 years apart (2004 and 2009, respectively), which, due to the technological progress along the time, led to rather significant differences in the two systems.

- The camera of the MAGIC I telescope consisted of 577 pixels (divided in small pixels, 1 inch diameter, in the inner part of the camera and large pixels, 2 inch diameter, in the outer part). The camera of MAGIC II consists of 1039 pixels, all small, 1 inch diameter.

- The trigger area of MAGIC II had an effective area of 1.66 times larger than the one of MAGIC I.
- MAGIC I readout was based on optical multiplexer and off-the-shelf FADCs (MUX-FADC [1]), which was robust and had an excellent performance but was expensive and bulky). The readout of MAGIC II was based on the DRS2 chip ¹ (compact and inexpensive but performing worse in terms of intrinsic noise, dead time and linearity compared to the MUX-FADC system).
- Receiver boards of MAGIC I, which are responsible for converting the optical signals into electrical ones, to split the signal into the analogue branch of the readout and the digital branch for the trigger, as well as to apply a Level-0 trigger condition (L0-trigger)² depending on the height of the signal in a trigger channel, were built using an old technology and were showing high failure rate (due to aging). This resulted in frequent problems in setting the discriminator thresholds (DTs) during the observations and only a rather slow reaction of the individual pixel rate control (IPRC), in order of several minutes, to adjust the DTs depending on the star field of the observations. This caused some loss of costly observation time. The receiver boards of MAGIC II allow instead a fast response (order of several seconds) of the IPRC thanks to a build-in FPGA and an easy and robust communication through the VME bus.

In years 2011-2012 MAGIC underwent a major upgrade program to improve and to unify the stereoscopic system of the two telescopes. This paper describes the main items of the upgrade and the commissioning of the upgraded MAGIC.

1. see <http://drs.web.psi.ch/>

2. The Level-0 trigger is a discriminator applied on a signal amplitude.

structure took also place to compensate the weight increase of the camera.

- Upgrade of the readout of the MAGIC I telescope from 577 to 1039 channels³.
- Upgrade of the L1 trigger of the MAGIC I telescope. The new trigger is a clone of the MAGIC II L1 trigger and has a 66% larger area than the previous trigger. The increase of the trigger area provides a more homogeneous gamma-ray efficiency across the camera, which is especially important for observations of extended sources and off-center observations.

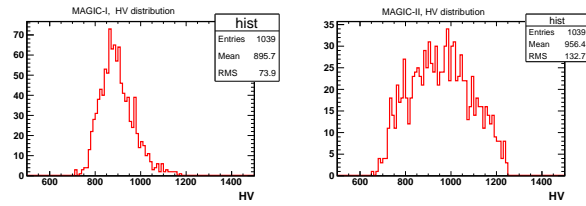


Figure 5: Distribution of the high voltages (HVs) applied to PMTs in MAGIC I and MAGIC II cameras after the charge flatfielding procedure. One can see that the HV distribution in the MAGIC II camera is wider. Maximal voltage which can be applied to the MAGIC PMTs is 1250 V.

In addition, two resting pillars were installed for the MAGIC I and MAGIC II cameras in Summer 2012. The cameras of the telescopes rest on top of the corresponding pillar while in the parking position, which greatly improves the stability of the telescope structure during storms, snow-fall and strong winds.

3 Commissioning of the system

The commissioning of the upgraded system required a dedicated, well experienced and highly motivated team of 5 to 10 physicists to stay on La Palma at the site of the experiment for a duration of several months after the installation of the hardware. The work has been mainly devoted to the following items:

Mapping of the channels. The 1039 pixels of the PMT camera have to be connected individually to the corresponding optical fibers at the camera side. The other ends of the fibers are then connected individually to the receiver channels. It is unavoidable that some mis-mappings take place. In order to correct mistakes, identify broken channels and other problems in the signal transmission, a dedicated pulse injection system of the camera is used. Artificial test pulses are generated at the base of the PMTs so that the whole signal transmission chain, including the trigger and readout, can be tested during the day.

L1 trigger check. The L1 trigger consists of 19 macrocells, each has 36 channels. Following logic algorithms are implemented: 2 next neighbor trigger (2NN), 3NN, 4NN, and 5NN. The L1 trigger is then programmed as an OR of the macrocells trigger. A dedicated hardware and software have been built to test all multiplicities. The L1 trigger systems of both telescopes have been extensively tested, hardware mistakes identified and repaired.

HV flatfielding. Each PMT has a different gain at a fixed

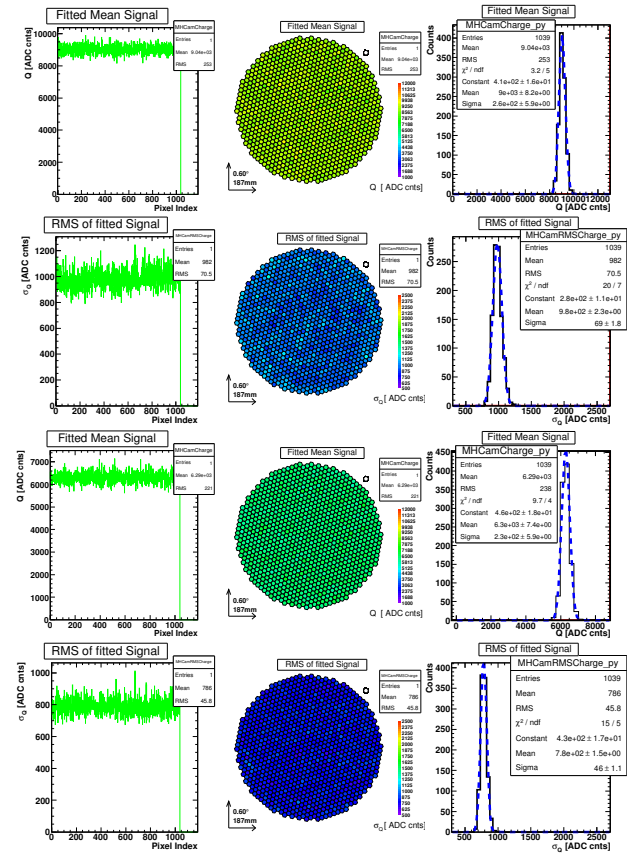


Figure 6: Charge distribution (mean and RMS) in MAGIC I (top) and MAGIC II (bottom) cameras after HV flatfielding for 2000 calibration pulses. Data from 22 October, 2012.

HV. The spread of the gains is unavoidable during the manufacturing process and is around 30-50%. The signal propagation chain introduces further differences in the gain: the optical links as well as the PIN diodes of the receivers mainly contribute to them. For the purpose of easier calibration of the signals, the HVs applied to PMTs are adjusted such that the resulting signal from calibration pulses (equal photon density at the entrance of the PMTs) is equal in all pixels when extracted after the digitization process. The resulting HV distribution for MAGIC I and MAGIC II cameras can be seen in Fig. 5. The distribution of the MAGIC I camera is narrower. This is due to the fact that during the construction of the MAGIC I camera the PMTs have been divided into two categories: those which have a higher gain than 30000 when applying 850 V and those with a lower gain. The ones with a higher gain are attenuated in the PMT base reducing the signal amplitude by a factor of two. This had the effect that the resulting gain and, therefore, also HV distributions are rather narrow. The quality of the HV flatfielding can be seen in Fig. 6 and stays constant with RMS/Mean at about 5-7% RMS for months.

L0 delays and L0 width adjustment. Due to the different light propagation times of the signals from the focal plane of the camera to the trigger system, the arrival times from different channels are slightly different (of the order of 2-3ns). This is mainly due to the differences in photo-electron

3. In the current configuration the readout can host up to 1152 channels per telescope

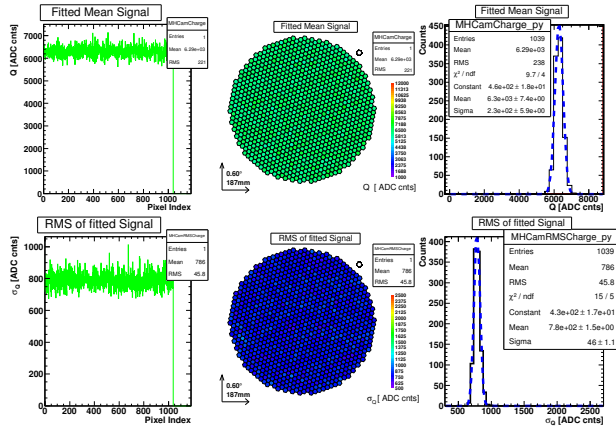


Figure 7: Rate scans taken changing discriminator thresholds to optimize the operating point of the MAGIC telescopes. Red (blue) points are L1 3NN rate scans taken with MAGIC I (MAGIC II) telescopes and the lines are analytical fits to them. The black points correspond the resulting stereoscopic rate of the system. The operating point has been chosen around 4.5 phe per channel.

propagation time in the PMTs when applying different HVs. An L0 delay is implemented on the receiver boards for each trigger channel in order to equalize arrival times of the signals at the L1 trigger for photons arriving at the same time at the camera plane. A dedicated hardware and software has been built to adjust the L0 delays automatically within several minutes. The delays are adjusted by injecting signals in each trigger pixel combination (e.g. every 3NN combination) and varying the delays of the pixels to identify the parameter space producing valid macrocell trigger signals. Finally the delays are set to the best values obtained from this scan. A minimum L0 signal width, which gave consistent results for all trigger channels, has been identified to be between 3ns to 5.5ns FWHM per pixel. In order to be on the safe side, all L0 trigger widths are then set to 5.5ns FWHM. The resulting gate of the L1 trigger is about (6 ± 0.5) ns.

Discriminator threshold (DT) calibration The DTs of the trigger channels (L0 trigger) are adjusted such that the sensitivity of the channels is flat in terms of photon density of Cherenkov photons. This is achieved by means of a rate scan over the range of DTs for each trigger channel when firing short (FWHM < 2 ns) calibration pulses with a given photon density (e.g., equivalent to a mean of 100 photoelectrons (phe) per pixel of the PMT camera). Then, for each trigger channel the required DT is determined, at which half of the calibration pulses is accepted, and the other half is rejected. In such a way, the DTs are calibrated in terms of phe's. We then scale the DTs linearly to obtain a DT for a desired phe level. As there are some small differences between the analogue and digital signal chains, and the DT is applied to the amplitude, whereas the HV flatfielding is done for the integrated signal, there is some 10% spread of the resulting DTs (pixel-to-pixel).

Adjusting the operating point of the trigger Rates scans have been performed at clear nights at low zenith angles to determine what is the shape of the trigger rate as a function of the DTs in phe. Mono rate scans as well as stereoscopic rates scans have been performed and the performance has been shown to be stable for several nights. An example of

the rate scans is shown in Fig. 7. One can see the steep slope of the rate at low DTs, where the rate is dominated by the chance coincidence. At higher DTs, the trigger rate is dominated by the rate of the cosmic ray showers. One can see that the coincidence trigger (stereo trigger) is strongly suppressing the chance coincidence triggers. The operating point for MAGIC has been chosen to be around 4.5 phe, resulting in a stereo rate of around 280 Hz, whereas around 40Hz out of it is a chance coincidence trigger.

Individual pixel rate control (IPRC) The flatfielded DTs may result in very different individual pixel rates (IPRs, measured on the receiver boards) during the operation since a) the spectral sensitivity of PMTs is different and b) the rates depend on the sky region the pixel is exposed to (e.g. it may contain stars, which would increase NSB fluctuations and, therefore, the IPR). As long as the IPRs are between 300kHz and 1.1MHz (mean being around 800kHz), no action is taken. For IPRs outside of these programmable limits, a IPR control software takes care of increasing or decreasing of the DTs for the affected pixels in order not to spoil the resulting L1 telescope rate.

The performance of the upgraded system can be found in [4, 3]. In addition to the upgrade as described in these proceedings, we are planning to install a complementary trigger system, dubbed *sumtrigger*, which has a lower energy threshold and will operate parallel to the existing L1 digital trigger [5].

4 Conclusions

A major upgrade of the MAGIC telescopes took place in the last two years. The commissioning of the upgraded system successfully finished in October 2012 and the telescopes restarted regular operation. Besides an improvement of the sensitivity (due to lower electronic noise in MAGIC II, more homogeneous trigger response and a larger trigger area of the MAGIC I camera as well as due to the reduction of the dead-time), the main goals of this upgrade were to secure stable performance and operation of the telescopes for the next 5-7 years. The expectations concerning the sensitivity and the stability of the instrument were fulfilled [3].

Acknowledgment: We would like to thank the Instituto de Astrofísica de Canarias for the excellent working conditions at the Observatorio del Roque de los Muchachos in La Palma. The support of the German BMBF and MPG, the Italian INFN, the Swiss National Fund SNF, and the Spanish MICINN is gratefully acknowledged. This work was also supported by the CPAN CSD2007-00042 and MultiDark CSD2009-00064 projects of the Spanish Consolider-Ingenio 2010 programme, by grant 127740 of the Academy of Finland, by the DFG Cluster of Excellence "Origin and Structure of the Universe", by the DFG Collaborative Research Centers SFB823/C4 and SFB876/C3, and by the Polish MNiSzW grant 745/N-HESS-MAGIC/2010/0.

References

- [1] H. Bartko, F. Goebel, R. Mirzoyan, W. Pimpl, & M. Teshima, 2005, NIM A, 548, 464.
- [2] M. Bitossi, R. Paoletti and D. Tescaro, 2013, to appear in IEEE Transactions on Nuclear Sciences.
- [3] J. Sitarek, M. Gaug, D. Mazin et al., NIMA in press, 2013, arXiv:1305.1007
- [4] J. Sitarek, E. Carmona, P. Colin et al., 2013, Proc. of the 33rd ICRC, Rio de Janeiro, Id. 0074.
- [5] J. Garcia Rodriguez et al., 2013, Proc. of the 33rd ICRC, Rio de Janeiro, Id. 666.